Transboundary and Emerging Diseases

WILEY

ORIGINAL ARTICLE

Risk assessment of imported COVID-19 in China: A modelling study in Sichuan Province

Lei Zhang[1,2] | **Lu Zhang**[3] | **Li Lai**[3] | **Zhanwei Du**[4,2] | **Yuling Huang**[5] | **Jianming Su**[6] | **Canglang Wu**[7] | **Shujuan Yang**[2,8] | **Peng Jia**[9,2]

[1]School of Cyber Science and Engineering, Sichuan University, Chengdu, China

[2]International Institute of Spatial Lifecourse Health (ISLE), Wuhan University, Wuhan, China

[3]College of Mathematics, Sichuan University, Chengdu, China

[4]School of Public Health, LKS Faculty of Medicine, The University of Hong Kong, Hong Kong, China

[5]Sichuan Center for Disease Control and Prevention, Chengdu, China

[6]Health Commission of Sichuan Province, Chengdu, China

[7]Health Information Center of Sichuan Province, Chengdu, China

[8]West China School of Public Health and West China Fourth Hospital, Sichuan University, Chengdu, China

[9]School of Resource and Environmental Sciences, Wuhan University, Wuhan, China

Correspondence
Peng Jia, School of Resource and Environmental Sciences, Wuhan University, No. 129 Luoyu Road, Wuhan 430079, China.
Email: jiapengff@hotmail.com

Shujuan Yang, West China School of Public Health and West China Fourth Hospital, Sichuan University, No. 16, Section 3, Ren Min Nan Road, Chengdu 610041, China.
Email: rekiny@126.com

Abstract

The importation of COVID-19 cases in China is due to the returning of Chinese citizens abroad, where the majority of cases stand. This study aimed to evaluate the risk of importing COVID-19 into the Sichuan Province of China and conduct a short-term risk prediction assessment and analysis. Data on COVID-19 cases in each country and Sichuan were collected, as well as visitors to Sichuan, population, area, and medical resources in each city in Sichuan province. According to different control strategies of entry aviation and quarantine control, we built models of epidemic transmission to estimate the risk for imported COVID-19 cases in 21 cities of Sichuan. Within 140 days of the policy change's implementation, the number of susceptible, infected, and recovered people in all cities followed the same pattern over time: (1) the number of susceptible people declined slowly at first, then accelerated to reach a stable value; (2) the number of infections gradually increased to a peak, then decreased; and (3) the number of recovered patients gradually increased to a stable value. Under the four different scenarios, there were no significant differences between the risk peaks because the social distance did not change. However, the peak time would be delayed due to the implementation of flight control and nucleic acid detection measures. The improvement of foreign epidemics (reduction of attenuation factors) all delayed the arrival of the peak risk value in Chengdu by about 20 days; however, the size of the peak value did not change significantly. The improvement of nucleic acid detection accuracy delayed the arrival of the peak risk value in Chengdu, but the size of the peak value did not change significantly. Therefore, flight control and the improvement of nucleic acid detection accuracy and overseas epidemic situations have positively affected the prevention and control of the epidemic in Sichuan.

KEYWORDS
COVID-19, imported case, risk assessment, SIR model

1 | INTRODUCTION

Coronavirus disease 2019 (COVID-19), caused by severe acute respiratory syndrome coronavirus 2 (SARS-CoV-2), has rapidly spread to more than 200 countries worldwide since its outbreak (Zhang et al., 2020; Zhou et al., 2020). The World Health Organization (WHO) declared COVID-19 a pandemic on 11 March 2020 (TIME, 2020). In China, the outbreak was first identified in December 2019 (Valentina et al., 2020). After a series of effective non-pharmaceutical interventions, including city lockdown, as well as different types and levels of emergency responses and prevention measures in other provinces and cities, the spread of COVID-19 was gradually contained with a declining incidence rate in China since 6 March 2020 (Lai et al., 2020). However, importation has become the primary source of infection in China as COVID-19 was increasingly prevalent in other countries, and overseas Chinese citizens returned home successively (Shen et al., 2020). As of 31 May 2020, the cumulative number of COVID-19 cases exceeded 5.9 million globally (World Health Organization 2020), and 1731 imported cases from 50 countries have been reported by the National Health Commission of China (National Health Commission of the People's Republic of China 2020). On average, there have been 54 infections a day between 1 April and 31 May, most of which were imported cases and subsequent second-generation cases (National Health Commission of the People's Republic of China 2020). The risk of local transmission brought by imported cases has become widespread (National Health Commission of the People's Republic of China 2020). Almost the entire population of China were still susceptible to COVID-19, and imported cases may lead to its re-emergence. The main cause is international flights, and ultimately opening them up will pose a massive challenge to domestic epidemic prevention. Therefore, understanding the effectiveness of international aviation control and its effect on the dynamic patterns of COVID-19 is of significant importance.

Some researchers have paid attention to the effect of population migration on the spread of COVID-19 (Zhang et al., 2020, Lai et al., 2020, Hu, Liu, et al., 2020, Wu, Leung, et al., 2020, Hu, He, et al., 2020, Hellewell et al., 2020, Wu, Ding, et al., 2020). Data from reported COVID-19 cases and Baidu Migration Index were used to construct and assess the risk model (Hu et al., 2020, Wu et al., 2020). Rather than the modelling and analysis of domestic epidemic spread conducted by previous research (Zhang et al., 2020, Lai et al., 2020, Hu et al., 2020, Hellewell et al., 2020), this study focuses on assessing and predicting local risk by imported cases. More input parameters, specifically asymptomatic infections, flight passenger entry data, and various city age distribution and medical conditions, are introduced in the modelling to improve the model's universality further. The epidemic data of COVID-19 in nine foreign countries and Zhejiang Province were collected to evaluate the risk of COVID-19 cases from aboard to Zhejiang Province (Wu et al., 2020). Elements of risk assessment and analysis were added when predicting and evaluating the risk of cities in the province. The propagation power model for mathematical modelling was also introduced, from which risk prediction analysis under dif-

ferent prevention and control measures can be performed. Previous research used disease incidence data from China and air travel passenger movements between China and Australia during and after the epidemic peak in China, derived from incoming passenger arrival cards, to test the impact of travel bans on epidemic control (Valentina et al., 2020). This study instead models based on individual COVID-19 case data, population density, medical conditions, and other model parameters to improve the accuracy and universality of model evaluation and prediction.

This study focuses on risk assessment of imported COVID-19 cases, specifically in Sichuan Province. Sichuan consists of 21 cities (Figure 1) and has the fourth largest population among other Chinese provinces, with a total of 83.75 million registered citizens as of 2019. Since the first incidence of COVID-19 was confirmed on 21 January 2020, 575 cases have been confirmed in the province between then and 31 May, ranking it 15th amongst Chinese provinces. The first imported case was reported on 17 March, and a total of 37 imported cases have been reported until 31 May. The non-pharmaceutical interventions for overseas travellers were also changed from only nucleic acid detection to including isolation for 14 days and even stricter aviation control. However, with the dynamic changes of the COVID-19 epidemic and diverse variations in demographic characteristics and flights from different countries, the risk of imported cases in Sichuan is unknown. The impact of the deregulation of international aviation on the future epidemic situation is still unclear. A discrete age-structured Susceptible, Infected, Recovered (SIR) model based on a previous study was established, taking into account the age profile of susceptibility to infection with imported cases as the foundation to forecast the epidemic trend, using reported importation data (Zhang et al., 2020). Then, the population density and medical conditions were introduced to estimate the risk of importation per city in Sichuan. This study aimed to model the effect of different measures for overseas travellers, including nucleic acid detection, isolation, and aviation control, on the generated infections, epidemic peak, and risk indexes of cities in Sichuan based on the discrete age-structured SIR model with imported cases. This study would provide a practical reference for further non-pharmaceutical interventions to prevent COVID-19 imported cases and epidemics in China.

2 | MATERIALS AND METHODS

2.1 | Scene modelling

The imported COVID-19 cases from each country to each city of Sichuan from 7 March and 6 May in 2020 were obtained from the Working Group on Imported COVID-19 Prevention and Control, Provincial Expert Panel on COVID-19, Health Commission of Sichuan Province. Due to the severe domestic epidemic from 7 to 18 March, travellers from each country to each city of the province were relatively low. From the 19th to the 28th of March, the risk of a domestic epidemic is significantly reduced while foreign epidemics are grad-
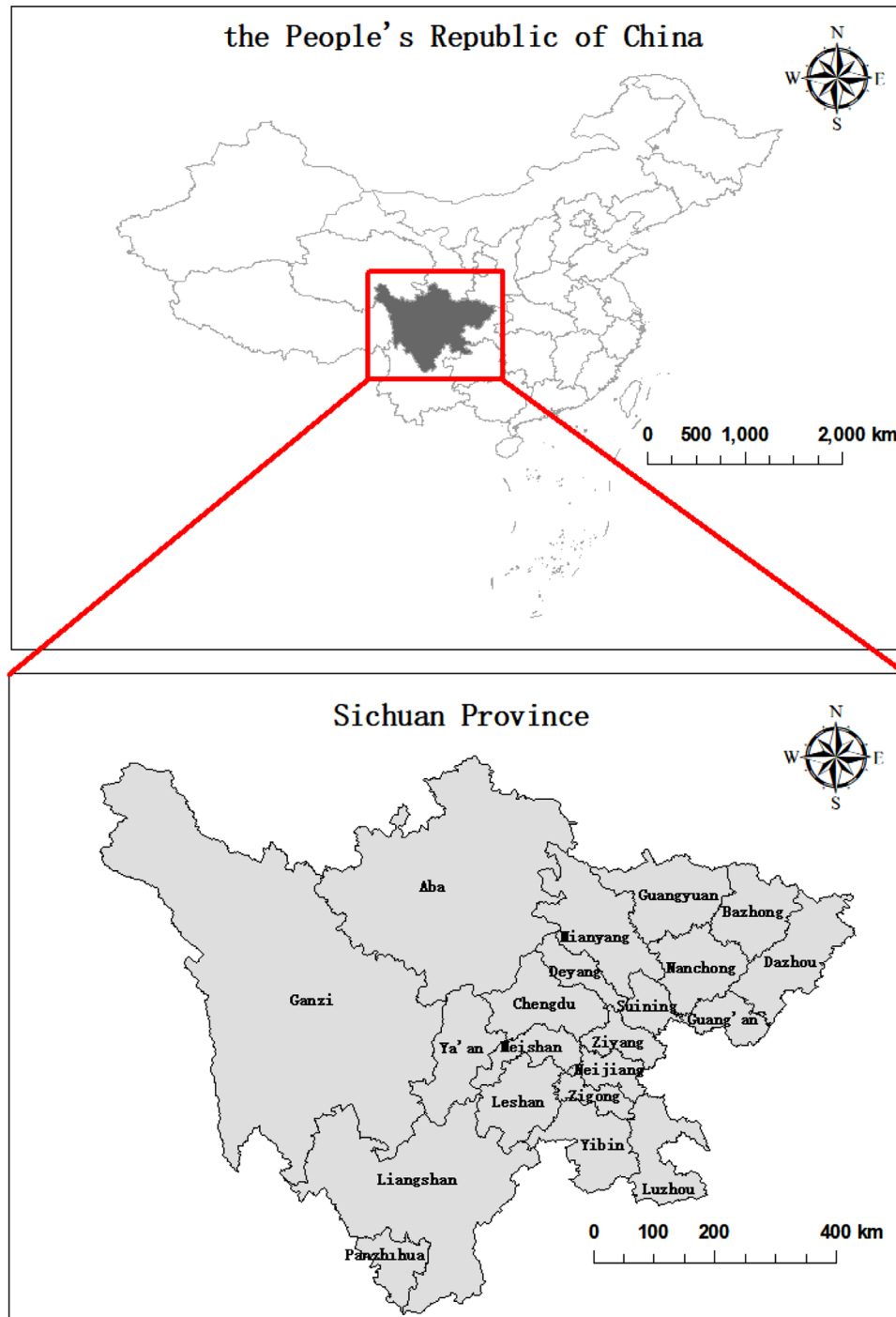
FIGURE 1 The map of all 21 cities in Sichuan Province, China

ually breaking out. After 29th March, Sichuan began to carry out overseas aviation control, significantly reducing the number of foreign visitors.

Sichuan also adopts a 14-day quarantine policy for foreign visitors. If this policy were eliminated, only COVID-19 nucleic acid tests would be performed; if a negative test, the visitor tested would be released into the local population. However, the detection accuracy of the test is 86%–98% (Udugama et al., 2020). The resultant accuracy suggests that

there is still a probability of incorrect detection, and infected overseas visitors with false negatives might cause an outbreak.

This study considers the impact of the two control policies of liberalizing inbound aviation and stopping isolations of visitors on the spread risk of COVID-19 in various cities of Sichuan. Specifically, this study forecasted and evaluated the transmission risk of COVID-19 caused by overseas importation after the change of policy in the following four scenarios: (1) no control on inbound aviation, not conducting

nucleic acid testing for inbound travellers, and releasing them directly into the local population; (2) no control on inbound aviation, conducting nucleic acid tests for inbound travellers, and releasing only those who tested negative into the local population; (3) the control of inbound aviation is still maintained, inbound travellers will no longer undergo nucleic acid testing, and they will be released directly into the local population; (4) the control of inbound aviation is still maintained and at the same time, inbound travellers will undergo nucleic acid testing and only those who are negative will enter the local population.

For Scenarios 1 and 2 (no aviation control), the data (including age, number of people, etc.) of visitors from various countries in Sichuan from 19 to 28 March were used as a periodic cycle to generate the data of visitors within 140 days (arbitrarily selected number to show the whole risk trend) from the date of policy change. For Scenarios 3 and 4 (aviation control is present), the data of the inbound travellers from various countries in Sichuan during the 10 days of 29 March to 7 April were cycled to generate the data within 140 days from the date of policy change. The number of infected imported people from each age group on each day was estimated by multiplying the weight of the imported people within 140 days of each age group by the prevalence rate and nucleic acid detection error probability of each country. The number of infectious individuals was input into the discrete age-structured SIR model to obtain the number of susceptible individuals, infectious individuals, and recovered individuals in various cities of Sichuan (Chengdu, Nanchong, Luzhou, Mianyang, Dazhou, Yibin, Liangshan, Guangyuan, Panzhihua, Deyang, and Suining). Subsequently, the SIR model also had the predicted value at risk within 140 days from the policy change date.

2.2 | Discrete age-structured SIR model with imported cases

As transmission intensifies in other countries, the interplay between age, contact patterns, social distancing, susceptibility to infection, and COVID-19 dynamics remains unclear. Therefore, considering the information described on age-structured contact patterns and susceptibility, a classic age-structured SIR model (Zhang et al., 2020) was used to simulate COVID-19 transmission dynamics and study the impact of the above factors on transmission. In this study, imported cases were introduced to the mentioned age-structured SIR model to study the total risk caused by imported cases of COVID-19 in an area from other countries.

Briefly, suppose there are four groups of people in an area: the susceptible (S), the infected (I), the recovered (R), and the imported (P). Each of the four groups is divided into fourteen 5-year age groups (0–4, 5–9, …, 60–64, 65+ years old). Susceptible individuals are exposed to an age-specific force of infection, regulated by the average number of contacts per day that individuals of a given age group have with individuals of all age groups. At the same time, the imported people (including susceptible or infected individuals) enter the city from other countries every day, in which the number of infected individuals is esti-

mated by the product of the total number of imported populations from a specific country and the prevalence rate of COVID-19 of that country. Thus, the following discrete age-structured SIR model is used to express the COVID-19 transmission dynamics with imported cases, which can be described by the following set of stochastic difference equations:

$$S_i[m+1] = S_i[m] - \beta \sum_{j=1}^{n} M_{ij} \frac{I_j[m]}{N_j[m]} \sigma_i S_i[m]$$

$$+ \sum_{k=1}^{K} (1 - \mu_k[m])(P_{ki}[m] + W_{ki}[m]),$$

$$I_i[m+1] = I_i[m] + \beta \sum_{j=1}^{n} M_{ij} \frac{I_j[m]}{N_j[m]} \sigma_i S_i[m]$$

$$+ \sum_{k=1}^{K} \mu_k[m](P_{ki}[m] + W_{ki}[m]) - \gamma I_i[m], \quad (1)$$

$$R_i[m+1] = R_i[m] + \gamma I_i[m],$$

where i represents the age group; $n = 14$ is the total number of age classes; $S_i[m]$ is the number of susceptible individuals in age group i on the m-th day; $I_i[m]$ is the number of infectious individuals in age group i on the m-th day; $R_i[m]$ is the number of recovered individuals in age group i on the m-th day; $P_{ki}[m]$ is the number of imported individuals in age group i from country k on the m-th day, which is assumed to be disturbed by Gaussian white noise $W_{ki}[m]$ with zero mean and deviation $\delta_{ki}[m] = P_{ki}[m]$. The total number of individuals in age class i is $N_i = S_i + I_i + R_i + P_i$.

In this study, the number of the (S, I, R) individuals in each age group was derived from the records in the Sichuan Center for Disease Control and Prevention. The number of imported individuals in each age group was derived from previous studies (Health Commission of Sichuan Province 2020, Chengdu Municipal Health Commission 2020), and the standard deviation of the imported individuals in each age group was estimated from the first two data. The meaning of parameters in the model is as follows: $\mu_k[m]$ is the prevalence rate of country k on the m-th day, the relevant data were derived from previous studies (Health Commission of Sichuan Province 2020, Chengdu Municipal Health Commission 2020); β is the transmission rate, of which its range interval [0.01495–0.05234] has been estimated in a previous study (Zhang et al., 2020), and the corresponding basic reproduction number R_0 is estimated to be in the range interval [1,3.5]; the percentage of asymptomatic cases is estimated to be about 31%–86% according to previous studies (Zhang et al., 2020, Nishiura et al., 2020); γ is the recovery rate. In the SIR model, the recovery rate is equivalent to the inverse of the duration of the generation time (Liu et al., 2018). Therefore, $1/\gamma$ is set to be 5.1 days (Zhang et al., 2020, Zhang et al., 2020); M_{ij} is the average number of contacts between individuals in age group i with individuals in age group j. The matrix of elements M_{ij} represents the contact matrices for regular weekdays and the COVID-19 outbreak period in Wuhan, estimated from a previous survey (Zhang et al., 2020); σ_i is the susceptibility to infection of individuals in age group i, which is given by the same study (Zhang et al., 2020).

2.3 | Total risk calculation

The risk index of COVID-19 on the m-th day to study the risk caused by imported cases of COVID-19 from other countries in a given area was estimated as follows:

$$Risk[m] = I[m]/Total\ medical\ resources, \qquad (2)$$

where $I[m] = \sum_{i=1}^{n} I_i[m]$ is the total number of infectious individuals on the m-th day of this area, calculated using the proposed discrete age-structured SIR model (1); the comprehensive medical resource is represented by the total number of hospital beds in that area.

2.4 | Statistical analysis

The data of COVID-19 cases in various countries, imported cases, total population, age structure, and medical resources of each city were sorted out and counted. The time trend of overseas imports from 7 March to 6 May was also analysed. The data, prediction trend, and risk index of the different kinds of individuals in various cities were processed in MATLAB 2017. The change trend and risk of the various individuals were also drawn in MATLAB 2017, and the risk map of overseas visitors in Sichuan (weighted population density) was drawn by Pyecharts.

3 | RESULTS

3.1 | Growth of numbers of (S, I, R) individuals caused by imported cases

The 95% confidence intervals and the mean of the totals of susceptible individuals, infectious individuals, and recovered individuals in all cities of Sichuan within 140 days after the changed policy under the four scenarios are shown in Figure 2. The total number of individuals in the cities without imported cases from 19 March to 7 April 2020 is not shown. We set the transmission rate β as the median of the interval, 0.0336, and the corresponding basic reproduction number R_0 was set as the median of the interval, 2.25. Following that, the percentage of asymptomatic cases was set as the median of the interval, 58.5%, while the nucleic acid detection accuracy was set as the median of the interval, 92%. As can be seen in Figure 2, under the four scenarios, the number of susceptible individuals, infectious individuals, and recovered individuals in each city showed the same trend within 140 days: the number of susceptible individuals first decreases slowly and then accelerates to a stable value; the number of infected individuals gradually increases to a peak and then decreases; the number of recovered individuals gradually increases to a stable value. The time and value of the peak of the infected population could be matched to the number of infectious individuals (Figure 2).

Then, Chengdu was taken as an example for analysis of the impact of the basic reproduction number R_0 on the COVID-19 epidemic. Figure 3 shows the 95% confidence intervals and the mean number of infectious individuals in Chengdu under different values of basic reproduction number R_0 over time when the percentage of asymptomatic cases was 31%, 58.5%, and 86% (minimum, median, and maximum values of the range [Zhang et al., 2020, Nishiura et al., 2020]). The accuracy of nucleic acid detection was fixed as the interval median, 92%. In particular, the number of $R_0 = 1$ is displayed in the locally enlarged view since its value is minimal. Table 1 also gives the maximum mean number of the infected population in Figure 3 with different basic reproduction numbers R_0 and the percentage of asymptomatic cases under the four scenarios in Chengdu.

It can be seen that at the same basic reproduction number R_0, the trend of infectious individuals over time was the same. It is also noticed from the peak value that the greater the percentage of asymptomatic cases, the earlier the arrival time of the peak value of infectious individuals. The basic reproduction number R_0 greatly influenced the trend of infectious individuals; even a slight increase in the rate can cause a considerable increase in infectious individuals. For the same percentage of asymptomatic cases, the higher the basic reproduction number R_0, the earlier and higher the peak of infectious individuals.

3.2 | Risk of COVID-19 (weighted population density) caused by imported cases

Figure 4 shows the changes in the 95% confidence intervals and the mean risk in each city of Sichuan over 140 days after the policy change under the four scenarios. The total number of people in the cities without overseas visitors from 19 March to 7 April is not shown. The basic reproduction number R_0 is taken as the median interval of 2.25, the percentage of asymptomatic people is taken as the median interval of 58.5%, and the nucleic acid detection accuracy rate is taken as the median interval of 92%. Moreover, Table 2 gives the maximum mean risk in each city in Figure 4 under the four scenarios. Figure 5 shows the heat map of the changes in the mean risk (weekly average) of each city in Sichuan over 140 days after the policy change under the four scenarios. Figure 6 shows the hierarchical display map of the peak of mean risk in each city of Sichuan under the four scenarios.

Next, Chengdu was taken as an example to analyse the impact of the basic reproduction number R_0 on the 95% confidence intervals and the mean risk of COVID-19 transmission, as shown in Figure 7. Table 3 gives the maximum mean risk of Figure 7 with different basic reproduction numbers R_0 and the percentage of asymptomatic cases under the four scenarios in Chengdu. Since the number of infectious individuals weights the risk of a given area to a fixed value (dividing population density by medical resources), the results, in this case, are consistent with the ones shown in Figure 3. In particular, the number of $R_0 = 1$ is displayed in the locally enlarged view since its value is minimal.
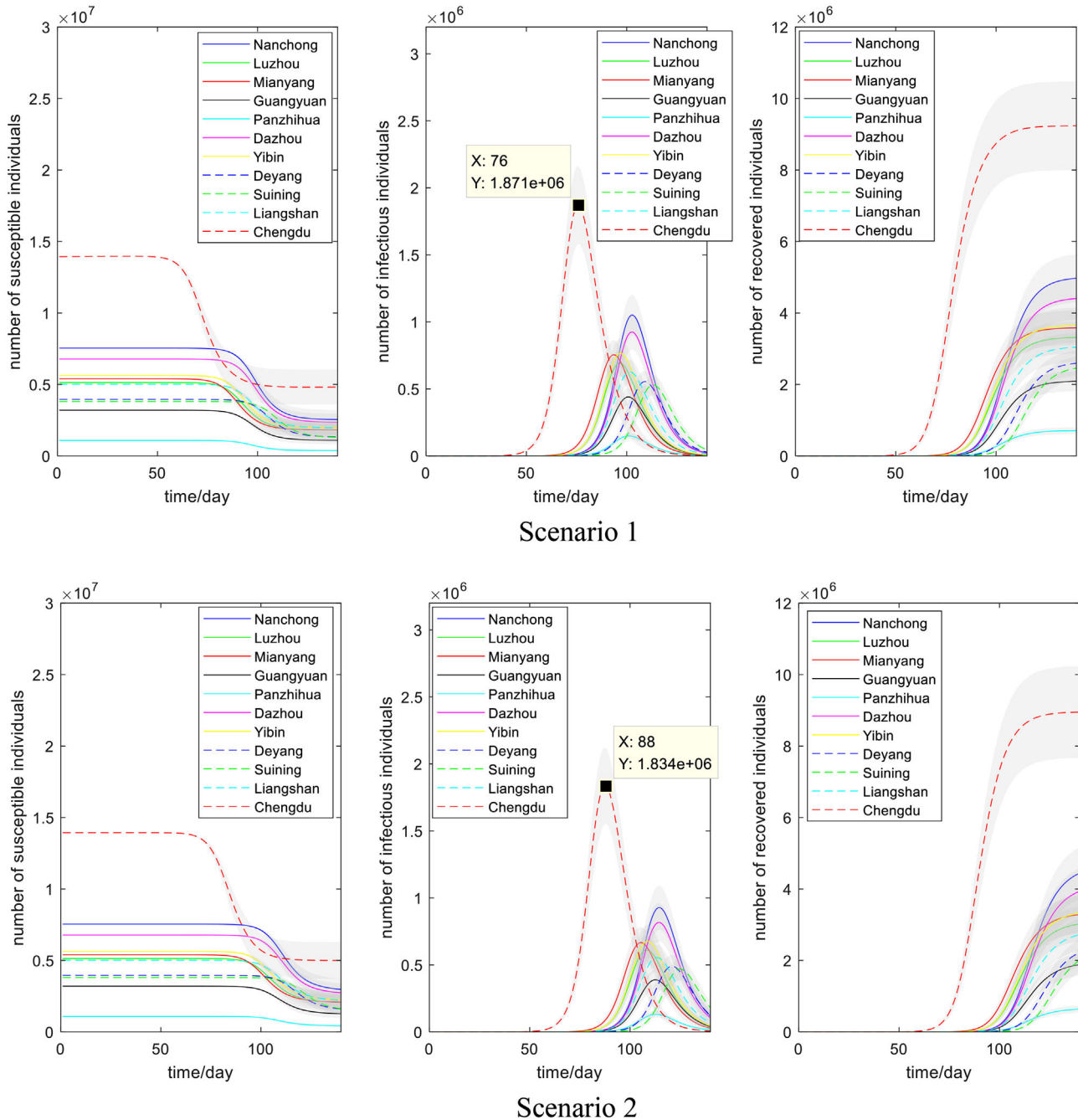
FIGURE 2 The 95% confidence intervals of the number of susceptible individuals, infectious individuals, and recovered individuals in various cities of Sichuan over time, projected in the four scenarios

3.3 | Influence of contact matrices on risk

Figure 8 shows the 95% confidence intervals and the mean risk before and after the social distance change in Chengdu in the four scenarios. The basic reproduction number R_0 is taken as the median value of 2.25, the percentage of asymptomatic people is taken as the median value of 58.5%, and the accuracy of nucleic acid detection is taken as the median value of 92%. It can be seen that in the four different scenarios, the peaks of the mean risk of scenarios

3 and 4 (with control on inbound aviation) are significantly smaller than those of scenarios 1 and 2 (no control on inbound aviation) (Figure 8a). Moreover, the peak arrival time will be delayed due to the implementation of aviation control and nucleic acid detection measures. Figure 8a,b shows that, given the same overseas input, a change in the social distance reduces risk significantly in Chengdu. It can then be deduced that maintaining a certain social distance has an essential and positive effect on preventing and controlling the epidemic.
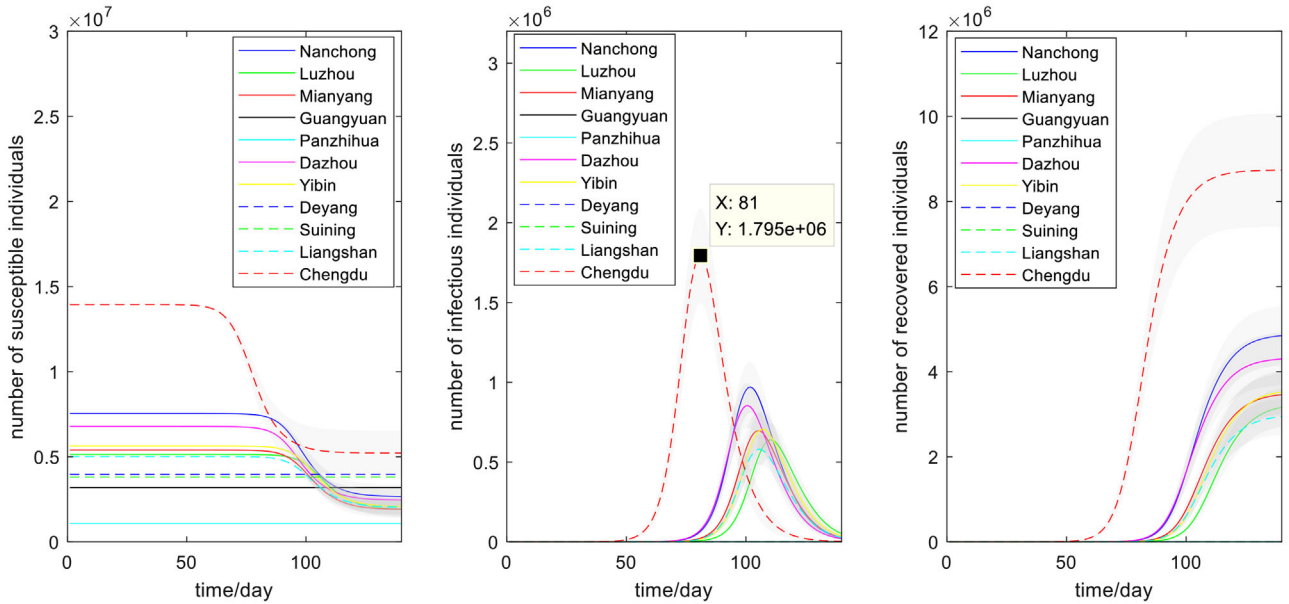
Scenario 3
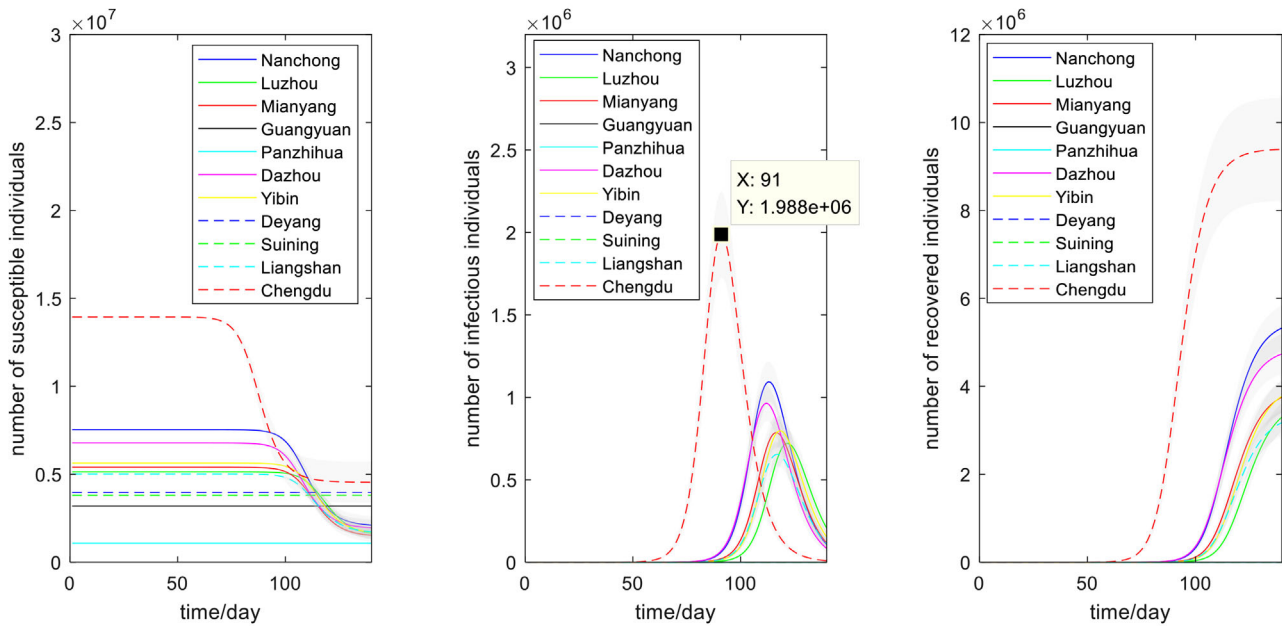
Scenario 4

FIGURE 2 Continued

3.4 | Influence of decay factor (overseas diagnosis rate) on risk

With the strengthening of foreign epidemic prevention and control, the epidemic situation in various countries is gradually under control. The overseas diagnosis rate (confirmed number/total number) will gradually decline. For this reason, introducing a decay factor to describe the change in overseas diagnosis rate is considered—the smaller the attenuation factor, the lower the diagnosis rate. Figure 9 shows the changes in the 95% confidence intervals and the mean risk of Chengdu

under the four different scenarios and different decay factors. The basic reproduction number R_0 is taken as the median value of 2.25, the percentage of asymptomatic people is taken as the median of the interval, 58.5%, and the accuracy rate of nucleic acid detection is taken as the median of the interval, 92%. As seen in the figure, under the four scenarios, the improvement of foreign epidemics (decrease of the decay factor) can delay the arrival of the risk peak in Chengdu. However, the size of the peak did not change significantly. Moreover, slight differences in the value and arrival time of the peak risk in the four scenarios are consistent with the results above (Figure 8a).
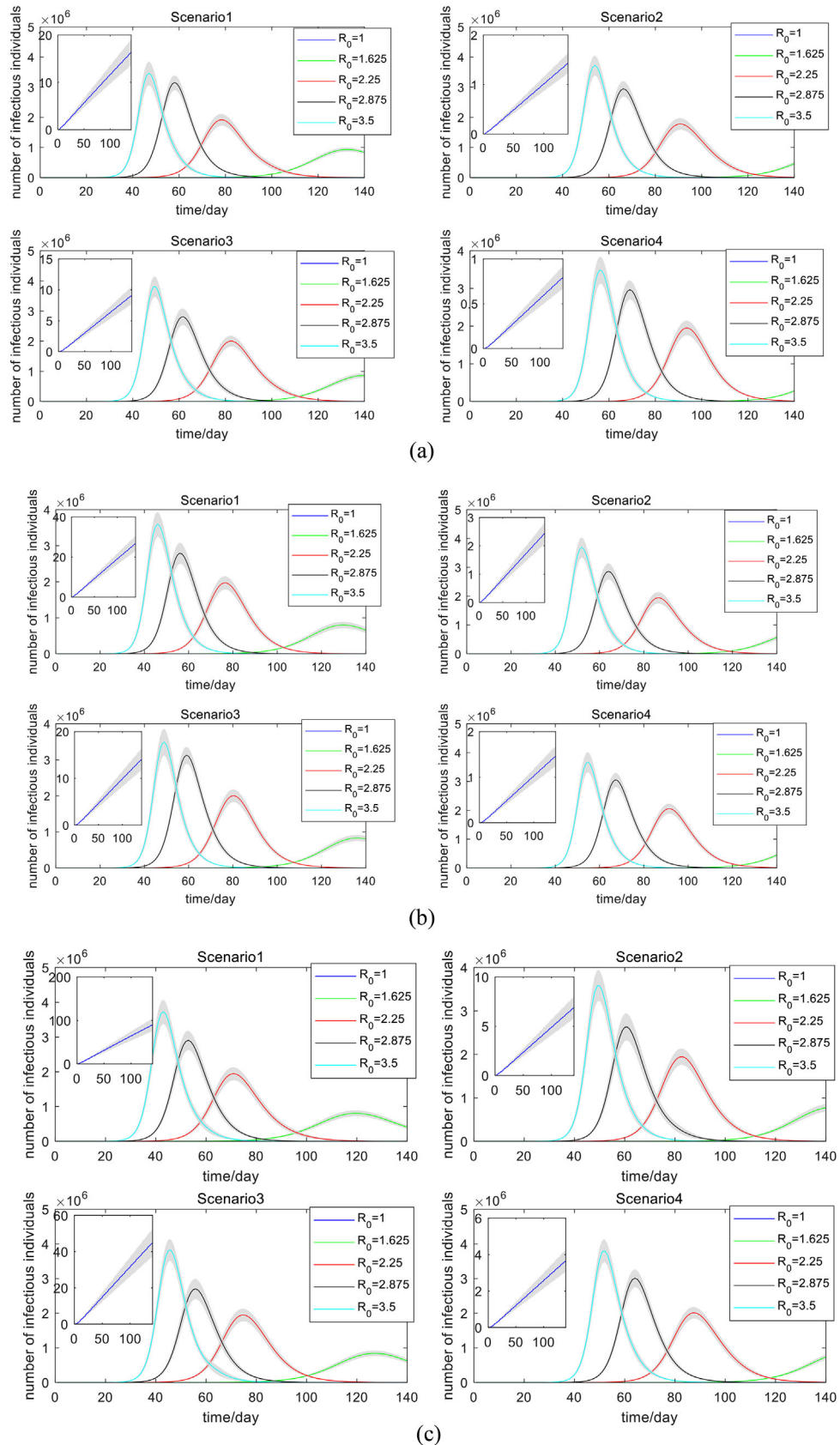
FIGURE 3 Under the four scenarios, the 95% confidence intervals of the number of the infected population in Chengdu were compared with different basic reproduction number R_0, and the percentage of asymptomatic cases is 31% (a), 58.5% (b), and 86% (c), respectively.

TABLE 1 Maximum mean numbers of the infected population in Figure 3 with different basic reproduction number R_0 and percentage of asymptomatic cases under the four scenarios in Chengdu

Scenario	Percentage of asymptomatic cases	$R_0 = 1$	$R_0 = 1.625$	$R_0 = 2.25$	$R_0 = 2.875$	$R_0 = 3.5$
1	31.0%	15	840,971	1,898,940	3,047,289	3,611,030
	58.5%	27	803,220	1,736,852	2,927,822	3,761,837
	86.0%	75	835,214	1,970,203	2,888,339	3,666,201
2	31.0%	1	522,545	2,036,335	2,716,607	3,950,633
	58.5%	2	630,874	1,852,089	2,913,019	3,679,652
	86.0%	7	821,439	1,952,149	3,066,943	3,571,804
3	31.0%	9	930,945	1,997,248	2,723,593	3,740,337
	58.5%	14	845,882	2,104,821	2,872,744	3,732,019
	86.0%	45	853,796	1,955,906	2,873,411	3,590,912
4	31.0%	0	308,579	1,949,861	2,948,941	3,456,909
	58.5%	1	399,762	1,991,968	2,652,363	3,665,599
	86.0%	3	701,266	1,815,262	3,023,445	3,590,129
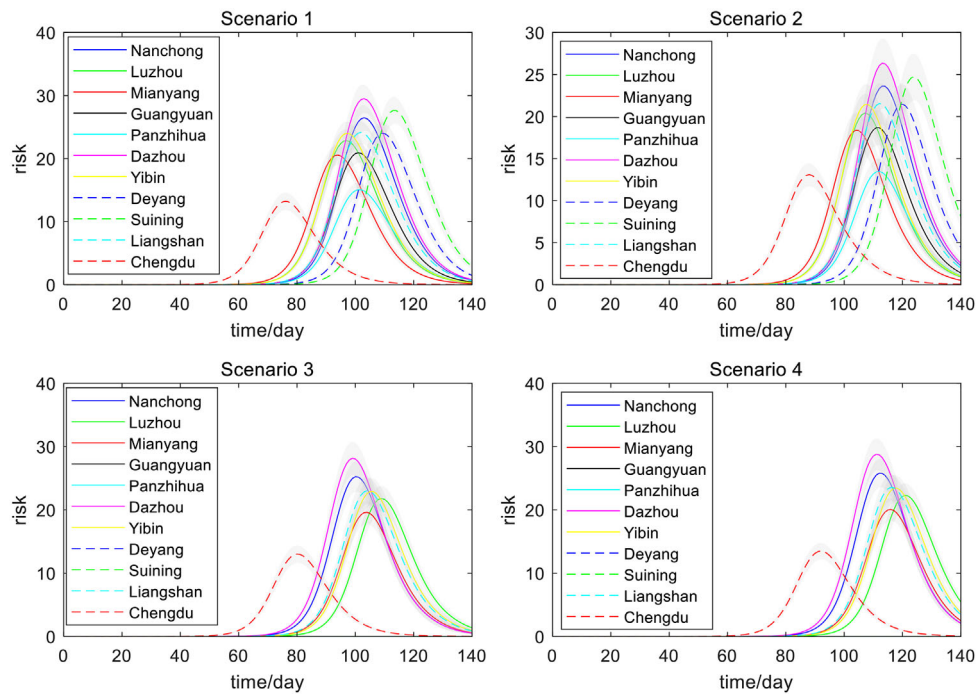
FIGURE 4 Trend of the 95% confidence intervals of risk in each city over time under the four scenarios

TABLE 2 Maximum mean risk in each city in Figure 4 under the four scenarios

City	Nanchong	Luzhou	Mianyang	Guangyuan	Panzhihua	Dazhou	Yibin	Deyang	Suining	Liangshan	Chengdu
Scenario 1	25.33	21.84	19.67	20.03	14.43	28.22	23.00	23.00	26.49	23.08	12.68
Scenario 2	25.28	21.82	19.68	19.98	14.40	28.16	22.92	22.96	26.44	23.03	13.74
Scenario 3	26.98	23.30	20.98	0	0	30.08	24.49	0	0	24.58	13.86
Scenario 4	22.85	19.71	17.78	0	0	25.47	20.72	0	0	20.83	13.10
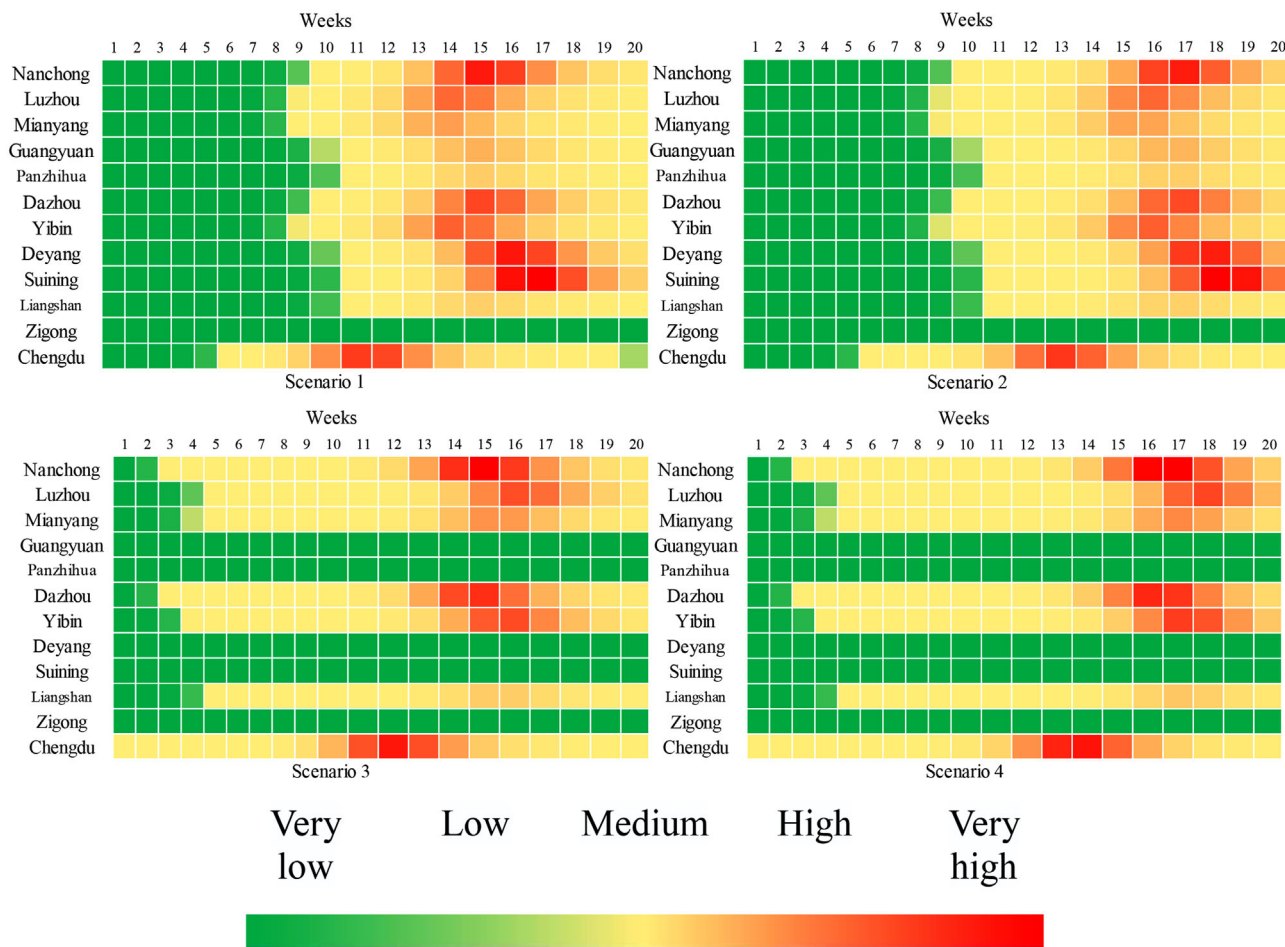
FIGURE 5 Trend of mean risk (average weekly) in each city over time under the four scenarios

TABLE 3 Maximum mean risk in Figure 7 with different basic reproduction number R_0 and percentage of asymptomatic cases under the four scenarios in Chengdu

Scenario	Percentage of asymptomatic cases	$R_0 = 1$	$R_0 = 1.625$	$R_0 = 2.25$	$R_0 = 2.875$	$R_0 = 3.5$
1	31.0%	0.11	5775.53	12,877.21	18,557.071	25,146.09
	58.5%	0.19	5755.06	12,622.29	20,703.67	25,268.74
	86.0%	0.52	5657.91	13,352.42	18,969.07	24,909.13
2	31.0%	0.01	3336.66	13,559.32	19,541.40	25,559.95
	58.5%	0.02	4418.11	13,570.36	21,494.80	23,293.47
	86.0%	0.04	5468.85	13,172.32	19,208.36	24,662.55
3	31.0%	0.06	5539.72	12,333.60	20,292.30	24,607.64
	58.5%	0.11	5378.60	12,286.70	20,455.47	24,332.61
	86.0%	0.28	5198.47	13,505.67	17,580.71	24,267.33
4	31.0%	0.005	1760.94	12,055.29	18,994.01	22,858.18
	58.5%	0.01	2438.22	13,125.94	18,131.11	23,331.59
	86.0%	0.03	4436.88	12,533.71	19,480.55	23,267.91
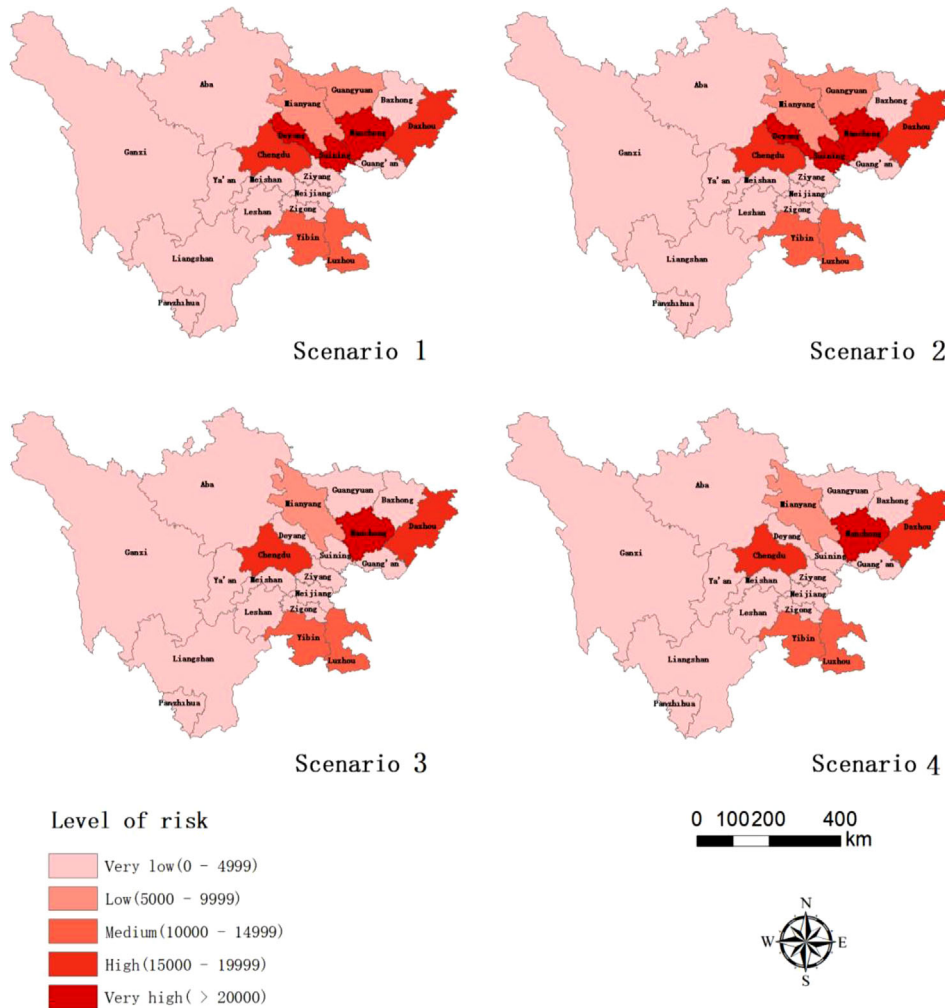
FIGURE 6 The mean risk peak grading map of each city under the four scenarios

3.5 | Change the probability of nucleic acid detection (weighted population density)

At present, the accuracy of nucleic acid detection for COVID-19 is between 86% and 98% (Udugama et al., 2020). The increased detection accuracy will play a positive role in preventing and controlling the epidemic. To this end, the impact of different nucleic acid detection accuracy rates on the risk in Chengdu is considered. Since Scenarios 1 and 3 do not perform nucleic acid detection, Figure 10 only shows the changes in the 95% confidence intervals and the mean of the risk in Chengdu at three different levels of the accuracy of nucleic acid detection under Scenarios 2 and 4. The basic reproduction number R_0 is taken as the median value of 2.25, and the percentage of asymptomatic people is taken as the median value of 58.5%. As seen, the increase in the accuracy of nucleic acid detection in both scenarios delays the arrival of the risk peak in Chengdu. However, the value of the peak did not change significantly. Consistent with the results above (Figure 8a), the value and arrival time of the peak risk in the two different scenarios are also slightly different. Moreover, to give more general results,

we reduced the accuracy of nucleic acid detection to 0.5 and 0.7. This reduction led to a lowered accuracy of nucleic acid detection, leading to the advance of peak arrival time.

4 | DISCUSSION

Flight management and control, adoption of nucleic acid detection and improvement of its accuracy, and improvement of foreign epidemics have positively affected the prevention and control of the epidemics in Sichuan. These efforts are mainly manifested in delaying the arrival of the peak risk. Transmission and recovery rates are the two major factors controlling the epidemic transmission trend. This study revised the contact matrices utilized by previous studies with an unchanged recovery rate and found that social distance significantly impacts epidemic prevention and control. This control is equivalent to reducing the transmission rate (or the basic reproduction number) while the recovery rate remains unchanged, thus greatly reducing the risk of transmission. Chengdu has the highest peak of infected individuals
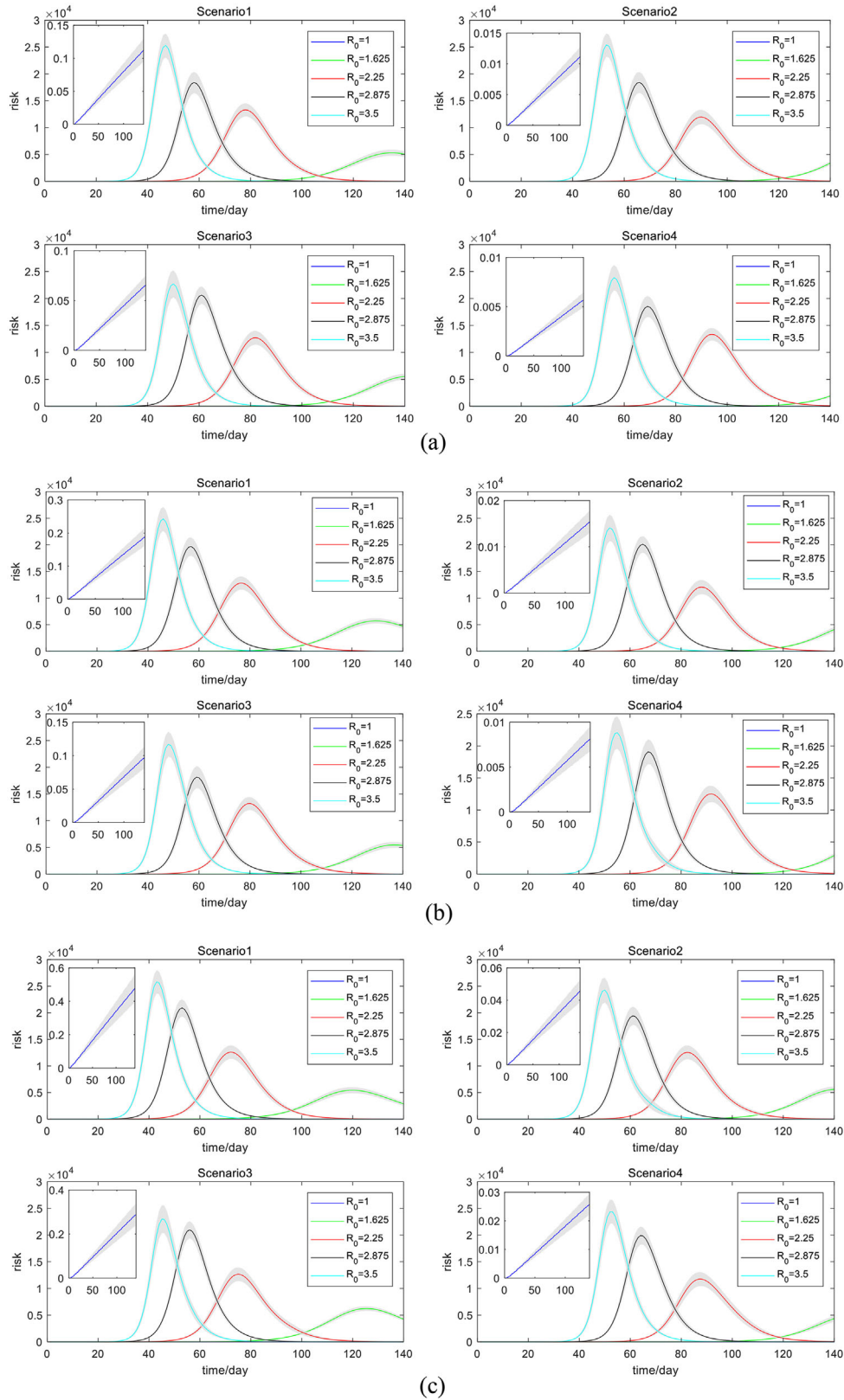
FIGURE 7   The 95% confidence intervals of risk and basic reproduction number R_0 over time under the four scenarios in Chengdu. The percentage of asymptomatic cases is 31% (a), 58.5% (b), and 86% (c), respectively.
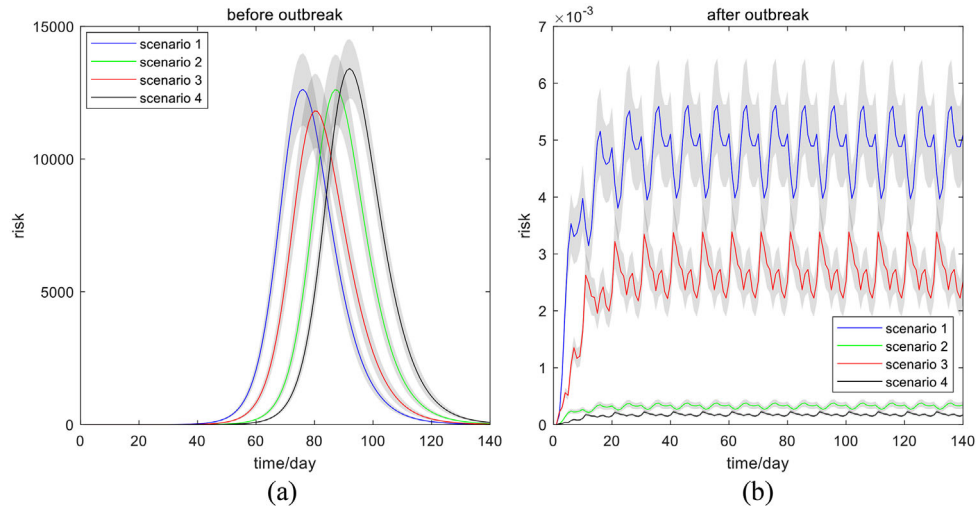
FIGURE 8 Comparison of the 95% confidence intervals of the risks in Chengdu over time after changing the exposure matrix in the four scenarios
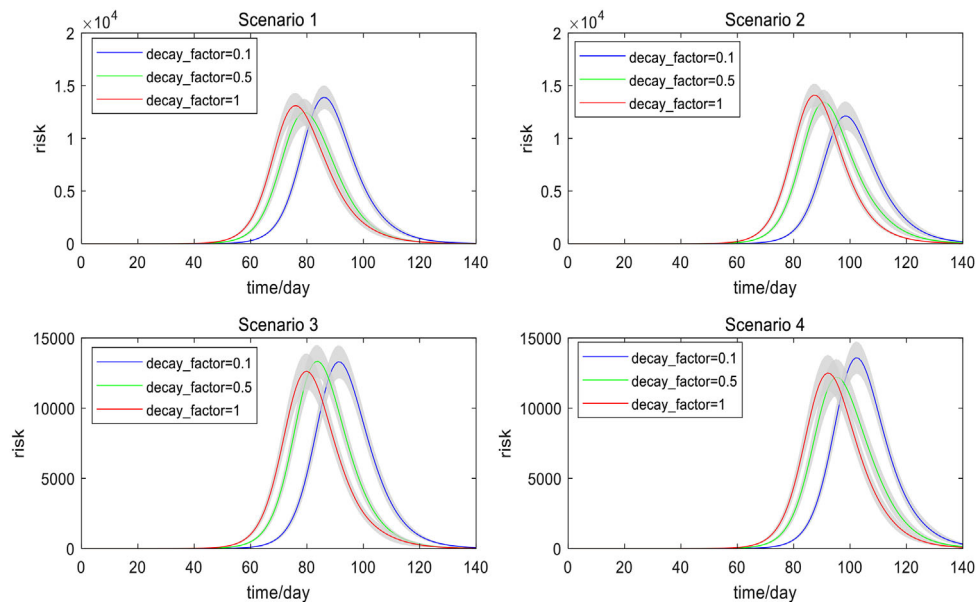
FIGURE 9 Comparison of the 95% confidence intervals of risks in Chengdu over time after changing the prevalence rate in the four scenarios

and was reached earliest among all the cities under the four scenarios (Figure 2). This high infection may be due to the large and continuous number of imported cases to Chengdu from various countries. In Scenarios 3 and 4, due to aviation control, there were no imported cases in Guangyuan, Panzhihua, Deyang, and Suining, and the number of infectious individuals was reduced to 0, so it was not shown.

It can be seen in these four scenarios that the risk of each city has a similar trend over time within 140 days: the risk gradually increases to the peak and then decreases (Figure 4). Both medical conditions and population density in different cities of Sichuan were considered at risk. For example, although Chengdu had the largest number of infectious individuals among all cities, medical conditions there were also

better than in other cities. The peak risk of Chengdu is the first to be reached but no longer the highest. In the four scenarios, the number of infectious individuals is the same, but due to different policies, each city's peak sizes and arrival times are slightly different (Figures 5 and 6). Although Suining and Deyang had few incoming travellers when aviation control was not implemented, their medical conditions were weak, and the population density was relatively high. Therefore, considering these factors, the risk of Suining and Deyang is higher than in other cities of Sichuan. After the implementation of aviation control, Guangyuan, Panzhihua, Deyang, and Suining have no overseas visitors, and the number of infectious individuals is reduced to 0. The risk is consequently also 0 and hence not shown.
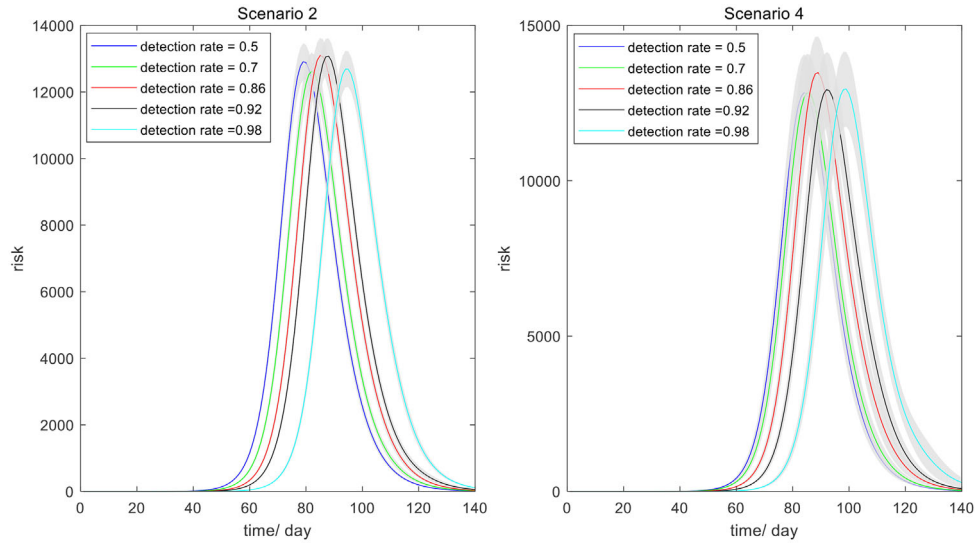
FIGURE 10 Comparison of the 95% confidence intervals of the risks in Chengdu over time after changing the accuracy of nucleic acid detection in Scenarios 2 and 4
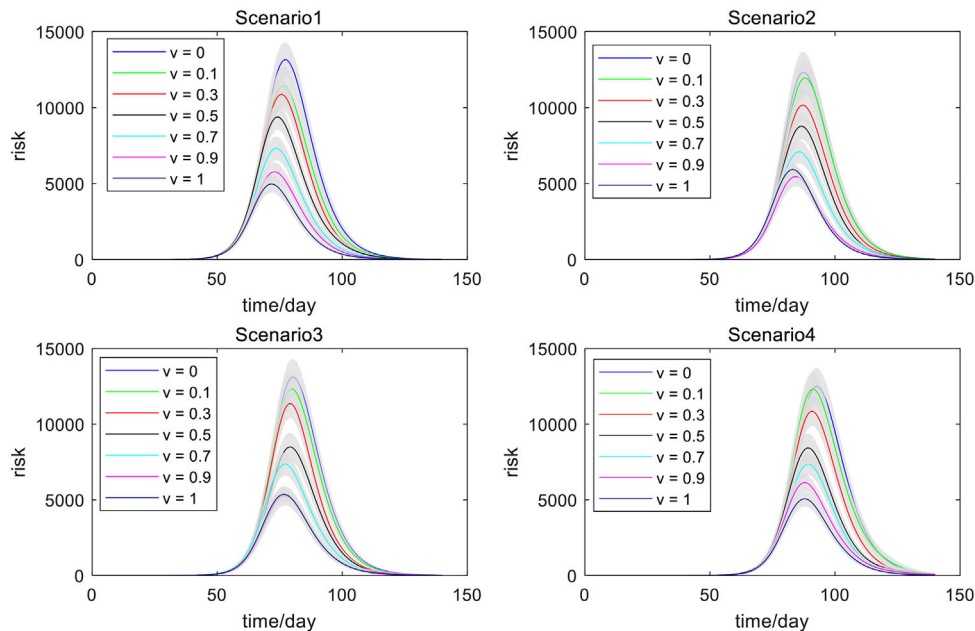
FIGURE 11 Comparison of the 95% confidence intervals of risks in Chengdu over time after changing the vaccine coverage *v* in the four scenarios

As of now, multiple COVID-19 vaccines are available. We also added the vaccinated individuals into the proposed model (1) to discuss the impact of vaccination on our proposed model. Figure 11 shows the changes in the 95% confidence intervals and the mean risk of Chengdu under the four different scenarios and different vaccine coverages, in which the vaccine coverage *v* in Sichuan was set as 0%, 10%, 30%, 50%, 70%, 90%, and 100%, respectively. The immunization rate of vaccinated individuals was hypothesized to be 0.6 (He et al., 2021). The basic reproduction number R_0 is taken as the median value of 2.25, and

the percentage of asymptomatic people is taken as the median value of 58.5%. The accuracy of nucleic acid detection is taken as the median value of 92%. It can be seen that the increase in the vaccine coverage in both scenarios delays the arrival of the risk peak in Chengdu and also reduces the peak value. Thus, vaccination can also effectively control the epidemic of COVID-19.

Moreover, the transmission rate has dramatically increased with the emergence of new variants of COVID-19. The basic reproduction number R_0 between the Omicron and the Delta variant ranges from 1.60
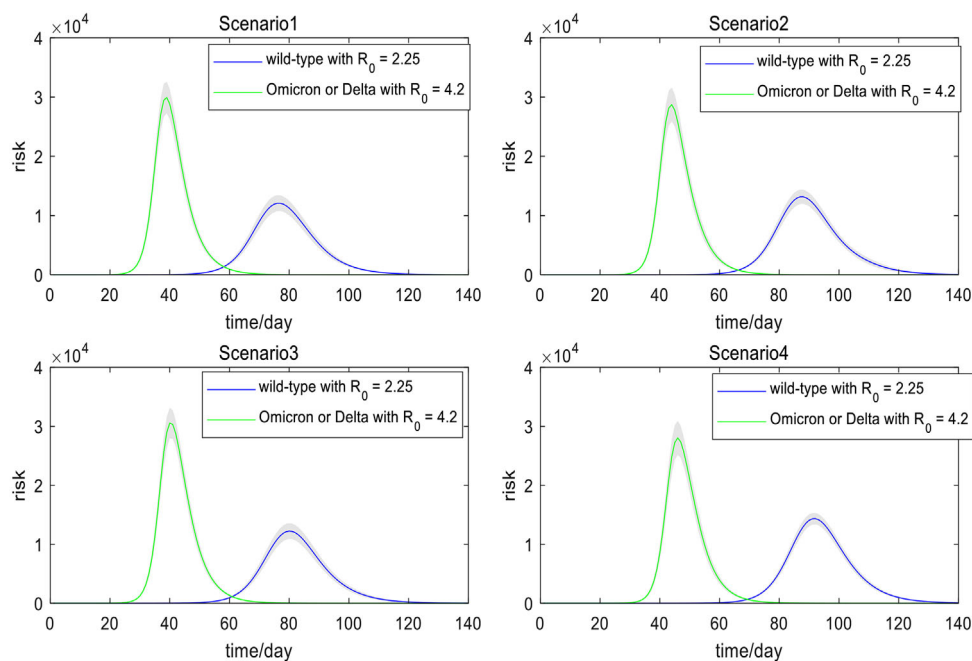
FIGURE 12 Comparison of the 95% confidence intervals of risks caused by different types of COVID-19 in Chengdu over time in the four scenarios

to 4.20, with a pooled estimate of 2.71 (95% confidence interval: 1.86, 3.56) (Du et al., 2022). However, the basic reproduction number R_0 in our study was supposed to be in the range interval [1, 3.5]. Furthermore, we also considered the case of Omicron or Delta with $R_0 = 4.2$. Figure 12 shows the changes in the 95% confidence intervals and the mean risk of Chengdu under the four different scenarios and different variants of COVID-19, that is wild type of COVID-19 with $R_0 = 2.25$ and Omicron (or Delta) with maximum $R_0 = 4.2$. The percentage of asymptomatic people is taken as the median value of 58.5%, and the accuracy of nucleic acid detection is taken as the median value of 92%. It can be seen that the arrival of the risk peak in Chengdu caused by the new variant with maximum $R_0 = 4.2$ is incredibly advanced, and the peak value is significantly increased.

After the COVID-19 outbreak, in addition to taking aviation control measures, the government advised the citizens not to gather and maintain social distance. Therefore, the contact matrices between the population underwent major changes before and after the COVID-19 outbreak. Given that the city scale and population flow in Chengdu and Wuhan are similar (Zhang et al., 2020), the contact matrices prior to and following the COVID-19 outbreak in Wuhan serve as the contact matrices before and after the Chengdu outbreak.

COVID-19-incubation-period cases and asymptomatic infections are still contagious, which adds an uncertain factor to the entry quarantine inspection. Also, this study predicted how the total number of infectious individuals would change if the control measures for imported individuals were changed. However, the real-world measures in Sichuan then were strict, resulting in an extremely low number of infectious individuals in the real situation, making it impossible to validate our model by comparing the simulated results to the real-world data. China still faces complex external pressure despite international

flight management and control and medical observation of visitors' isolation being centralized and strengthened. Especially in areas with relatively few medical resources that are under many challenges, maintaining social distance is very important. As the COVID-19 vaccine continues to be distributed, the following studies should focus on the risk assessment and prediction in the case of vaccine injection, virus mutation, and so forth, based on updated data sources and model optimization.

AUTHOR CONTRIBUTIONS

Peng Jia and Shujuan Yang conceived the idea and designed data analysis. Lei Zhang, Lu Zhang, Li Lai, and Zhanwei Du conducted the analysis. Yuling Huang, Jianming Su, and Canglang Wu contributed to data collection. Peng Jia and Shujuan Yang supervised the study. Lei Zhang, Lu Zhang, Li Lai, Shujuan Yang, and Peng Jia drafted the manuscript. All authors read and approved the final manuscript.

ACKNOWLEDGEMENTS

CONFLICT OF INTEREST

The authors declare no conflict of interest.

DATA AVAILABILITY STATEMENT

The data that support the findings of this study are available on request from the corresponding author. The data are not publicly available due to privacy or ethical restrictions.

ETHICS STATEMENT

The authors confirm that the ethical policies of the journal, as noted on the journal's author guidelines page, have been adhered to and the appropriate ethical review committee approval has been received.

REFERENCES

Chengdu Municipal Health Commission. (2020, January 21). *Epidemic notification*. http://cdwjw.chengdu.gov.cn/cdwjw/c135634/list.shtml

Du, Z., Hong, H., Wang, S., Ma, L., Liu, C., Bai, Y., Adam, D. C., Tian, L., Wang, L., Lau, E. H., & Cowling, B. J. (2022). Reproduction number of the omicron variant triples that of the delta variant. *Viruses*, *14*(4), 821.

He, X., Sun, X., Gong, F., Lin, J., Li, W., & Shenzhen Luohu Hospital Group. (2021). A cost-benefit analysis of the large-scale screening program for coronavirus disease-2019 (COVID-19) by nucleic acid test. *Modern Hospital*, *21*(9), 1403–1406.

Health Commission of Sichuan Province. (2020, January 21). *Epidemic notification*. http://wsjkw.sc.gov.cn/scwsjkw/gzbd01/ztwzlmgl_62.shtml

Hellewell, J., Abbott, S., Gimma, A., Bosse, N. I., Jarvis, C. I., Russell, T. W., Munday, J. D., Kucharski, A. J., Edmunds, W. J., Sun, F., & Flasche, S. (2020). Feasibility of controlling COVID-19 outbreaks by isolation of cases and contacts. *The Lancet Global Health*, *8*(4), e488–e496.

Hu, J., He, G. H., Liu, T., Xiao, J. P., Rong, Z. H., Guo, L. C., Zeng, W. L., Zhu, Z. H., Gong, D. X., Yin, L. H., & Wan, D. H. (2020). Risk assessment of exported risk of COVID-19 from Hubei Province. *Chinese Journal of Preventive Medicine*, *54*(4), 362–366.

Hu, J., Liu, T., Xiao, J. P., He, G. H., Rong, Z. H., Yin, L. H., Wan, D. H., Zeng, W. L., Gong, D. X., Guo, L. C., & Zhu, Z. H. (2020). Risk assessment and early warning of imported COVID-19 in 21 cities, Guangdong provinces. *Chinese Journal of Epidemiology*, *41*(5), 658–662.

Lai, S., Ruktanonchai, N. W., Zhou, L., Prosper, O., Luo, W., Floyd, J. R., Wesolowski, A., Santillana, M., Zhang, C., Du, X., & Yu, H. (2020). Effect of non-pharmaceutical interventions to contain COVID-19 in China. *Nature*, *585*, 410–413.

Liu, Q., Ajelli, M., Aleta, A., Merler, S., Moreno, Y., & Vespignani, A. (2018). Measurability of the epidemic reproduction number in data-driven contact networks. *Proceedings of the National Academy of Sciences of the United States of America*, *115*, 12680–12685.

National Health Commission of the People's Republic of China. (2020, May 31). *Epidemic notification*. http://www.nhc.gov.cn/xcs/yqtb/list_gzbd.shtml

Nishiura, H., Kobayashi, T., Miyama, T., Suzuki, A., Jung, S. M., Hayashi, K., Kinoshita, R., Yang, Y., Yuan, B., Akhmetzhanov, A. R., & Linton, N. M. (2020). Estimation of the asymptomatic ratio of novel coronavirus infections (COVID-19). *International Journal of Infectious Diseases*, *94*, 154–155.

Shen, S. P., Wei, Y. Y., Zhao, Y., Jiang, Y., Guan, J. X., & Chen, F. (2020). Risk assessment of global COVID-19 imported cases into China. *Zhonghua Liu Xing Bing Xue Za Zhi = Zhonghua Liuxingbingxue Zazhi*, *41*(10), 1582–1587.

TIME. (2020). *World Health Organization declares COVID-19 a 'pandemic.' Here's what that means*. https://time.com/5791661/who-coronavirus-pandemic-declaration/

Udugama, B., Kadhiresan, P., Kozlowski, H. N., Malekjahani, A., Osborne, M., Li, V. Y., Chen, H., Mubareka, S., Gubbay, J. B., & Chan, W. C. (2020). Diagnosing COVID-19: The disease and tools for detection. *ACS Nano*, *14*(4), 3822–3835.

Valentina, C., Heslop, D. J., & Raina, M. I. C. (2020). The effectiveness of full and partial travel bans against COVID-19 spread in Australia for travellers from China during and after the epidemic peak in China. *Journal of Travel Medicine*, *27*(5), taaa081.

World Health Organization. (2020, May 31). *Coronavirus disease 2019 (COVID-19) situation report – 132*. https://www.who.int/docs/default-source/coronaviruse/situation-reports/20200531-covid-19sitrep-132.pdf?sfvrsn=d9c2eaef_2

Wu, H., Ding, Z., Wu, C., Lu, Q., Li, F., & Lin, J. (2020). Risk assessment of COVID-19 cases imported from aboard to Zhejiang Province. *Preventive Medicine*, *32*(6), 541–545.

Wu, J. T., Leung, K., & Leung, G. M. (2020). Nowcasting and forecasting the potential domestic and international spread of the 2019-nCoV outbreak originating in Wuhan, China: A modelling study. *Lancet*, *395*(10225), 689–697.

Zhang, J., Litvinova, M., Liang, Y., Wang, Y., Wang, W., Zhao, S., Wu, Q., Merler, S., Viboud, C., Vespignani, A., Ajelli, M., & Yu, H. (2020). Changes in contact patterns shape the dynamics of the COVID-19 outbreak in China. *Science*, *368*(6498), eabb8001.

Zhang, J., Litvinova, M., Wang, W., Wang, Y., Deng, X., Chen, X., Li, M., Zheng, W., Yi, L., Chen, X., & Wu, Q. (2020). Evolving epidemiology and transmission dynamics of coronavirus disease 2019 outside Hubei province, China: A descriptive and modelling study. *The Lancet Infectious Diseases*, *20*(7), 793–802.

Zhou, M., Zhang, X., & Qu, J. (2020). Coronavirus disease 2019 (COVID-19): A clinical update. *Frontiers in Medicine*, *14*(2), 126–135.